

Institute of Physics and The Physical Society, London, 1965), p. 555.

¹⁰P. Grünberg, S. Hüfner, E. Orlich, and J. Schmitt, *Phys. Rev.* **184**, 285 (1969).

¹¹K. Aoyagi, K. Tsushima, and M. Uesugi, *J. Phys. Soc. Japan* **27**, 49 (1969).

¹²R. A. Buchanan, K. A. Wickersheim, J. J. Pearson, and G. F. Herrmann, *Phys. Rev.* **159**, 245 (1967); **159**, 251 (1967).

¹³D. A. Huchital and J. Dane Rigden, *Rev. Sci. Instr.* **39**, 1472 (1968).

¹⁴We wish to thank Dr. P. J. Kindlmann of Yale University for the design and construction of the digital photon counter.

¹⁵H. Winston and R. S. Halford, *J. Chem. Phys.* **17**, 607 (1949).

¹⁶R. Loudon, *Advan. Phys.* **13**, 423 (1964).

¹⁷M. Veyssie and B. Dreyfus, *J. Phys. Chem. Solids* **28**, 499 (1967).

¹⁸R. J. Elliott and R. Loudon, *Phys. Letters* **3**, 189 (1963).

¹⁹J. A. Koningstein and Toanng Ng, *Solid State Commun.* **7**, 351 (1969).

²⁰K. W. H. Stevens, *Proc. Roy. Phys. Soc. (London)* **A65**, 209 (1952).

²¹G. H. Dieke, *Spectra and Energy Levels of Rare Earth Ions in Crystals* (Interscience, New York, 1968).

²²C. W. Nielson and G. F. Koster, *Spectroscopic Coefficients for the p^n , d^n , and f^n Configurations* (MIT, Cambridge, Mass., 1964).

²³M. J. D. Powell, *Computer J.* **7**, 303 (1965); Harwell Subroutine Library Program No. VA02A.

²⁴B. G. Wybourne, *J. Chem. Phys.* **36**, 2301 (1962).

²⁵J. D. Axe, Jr., *Phys. Rev.* **136**, A42 (1964).

²⁶O. Sonnich Mortensen and J. A. Koningstein, *J. Chem. Phys.* **48**, 3941 (1968).

²⁷B. R. Judd, *Phys. Rev.* **127**, 750 (1962).

²⁸G. S. Ofelt, *J. Chem. Phys.* **37**, 511 (1962).

²⁹M. T. Hutchings and W. P. Wolf, *J. Chem. Phys.* **41**, 617 (1964).

³⁰J. A. Koningstein and G. Schaak, *Phys. Rev. B* **2**, 1242 (1970).

³¹A. Kiel and S. P. S. Porto, *J. Mol. Spectry.* **32**, 458 (1969).

³²J. A. Koningstein and O. S. Mortensen, *Phys. Rev.* **168**, 75 (1968).

³³K. Rajnak, *J. Chem. Phys.* **37**, 2440 (1962).

³⁴B. E. Argyle, R. L. Wadsack, and R. K. Chang, *ibid.* **42**, 1478 (1971).

Thermal Expansion of Rocksalt*

B. N. N. Achar[†] and G. R. Barsch

*Materials Research Laboratory and Department of Physics,
The Pennsylvania State University, University Park, Pennsylvania 16802*

(Received 5 November 1970)

The microscopic Grueneisen parameters and the temperature dependence of the thermal Grueneisen parameter of NaCl are calculated from a shell model with six parameters, five of which are taken as pressure dependent. All parameters are determined from experimental elastic, optical, and dielectric data at absolute-zero temperature. The results agree within 6–8% with experimental data. The discrepancy is primarily attributed to the experimental error of the input data that are used to determine the parameters of the model. Calculations have also been made for two versions of the rigid-ion model (RIM) which indicate that the apparent success previously attributed to the Kellermann model is mainly due to cancellation of errors arising from omitting second-nearest-neighbor interaction and electronic polarizability.

I. INTRODUCTION

While the caloric equation of state and the temperature dependence of the Debye temperature for NaCl have been extensively studied theoretically on the basis of the rigid-ion model (RIM) of Kellermann^{1,2} as well as several versions of the shell model^{3–6} (SM), for the thermal equation of state and the temperature dependence of the Grueneisen parameter γ , the only theoretical calculations available are based on the RIM.^{7–13} Moreover, the results of Arenstein *et al.*¹⁰ which are the only theoretical data for the temperature dependence of the Grueneisen parameter of NaCl are based on a

dubious procedure of determining the two repulsive parameters for the nearest-neighbor short-range interaction. These authors prefer to determine the repulsive parameters from the bulk modulus and the TO frequency and ignore the equilibrium condition. The results refer to a series of different values for the interatomic distance, and the quality of agreement with experimental data depends on the proper choice of one of these values. These "values have been corrected to the actual lattice spacing at each temperature" by Meincke and Graham¹¹ who find that the general shape of the γ vs T curve shows a minimum near 11 °K and agrees qualitatively very well with their own experimental values, but that

the theoretical data above the minimum are up to 10% higher than the experimental results. On the other hand, Barron *et al.*⁹ determine for NaCl and KCl the volume derivatives of the moments of the frequency spectrum $\gamma(n)$ [see Eq. (5.1) below] from the experimental thermal expansion data of Rubin *et al.* and of White,¹⁴ and find fair agreement with theoretical data based on the Kellermann model in connection with the equilibrium condition and with acceptable values of the remaining repulsive parameter. Except for the investigations of Fletcher and Powell¹² and of Morley,¹³ the above-mentioned theoretical treatments are based on the quasi-harmonic approximation¹⁵ and neglect the anharmonic contribution arising from thermal expansion by using temperature-dependent input data for the determination of the repulsive parameters. The primary objective of the papers of Fletcher¹² and of Morley¹³ is to study the anharmonic effects on thermal expansion at high temperature, and since the results are presented in the form of volume vs temperature data they do not yield accurate information on the Grueneisen function $\gamma(T)$ and are not suitable for studying the effect and limitations of the lattice dynamical model underlying the theoretical calculation.

For two other alkali halides, NaI and KBr, Cowley and Cowley¹⁶ have calculated the microscopic Grueneisen parameters (mode γ 's) and the temperature dependence of the macroscopic Grueneisen parameter from a simplified version of the SM. The agreement of their results with experimental data is good for NaI at low temperatures ($T/\Theta = 0.1$ to 0.2, where Θ = Debye temperature), but for both materials the theoretical results are about 20% too high at high temperatures ($T > \Theta$). It is somewhat surprising that a better theoretical model seems to give not as good agreement for the general shape of the γ vs T curve than the RIM.

In view of this situation, questions concerning the quality of the RIM arise. How good an approximation is the RIM for the Grueneisen parameter and its variation with temperature? Is its apparent success real or caused by a cancellation of errors due to various approximations? Can the agreement between theory and experiment be improved by using an appropriate version of the SM? Do anharmonic effects become important at intermediate temperatures ($T \approx \Theta$)?

The main objective of the present paper is to present answers to these general questions for NaCl and, in addition, to establish theoretically the shape of the Grueneisen function $\gamma(T)$ for NaCl at low temperatures, which is at present still open to controversy. While Meincke and Graham¹¹ and Barron *et al.*⁹ in an earlier paper suggest the existence of a low-temperature minimum of γ vs T near 11 °K, White¹⁷ assumes that γ levels off below this tem-

perature, and Barron and Batana¹⁸ conclude in a recent paper that "an appreciable" low-temperature minimum is highly unlikely. Barron's conclusion, however, is based on the RIM with nearest-neighbor central forces. Since it is known^{19,20} that inclusion of second-nearest-neighbor interaction strongly affects the pressure derivative of the shear modulus c_{44} and of the limiting value of the Grueneisen parameter at $T = 0$ °K, one must expect that the second-nearest-neighbor interaction will also alter the mode γ 's in the dispersive range, especially those of the TA branch in the [100] direction, which should already contribute to the temperature dependence of γ near 11 °K. In addition, these modes depend on the electronic polarizability, which is neglected in the RIM. Since both contributions to the mode γ 's are dependent on wave number, their effect on the macroscopic Grueneisen parameter will be temperature dependent, and it is therefore conceivable that this may cause a minimum at low temperature. It is therefore another objective of this paper to reinvestigate the existence of the minimum on the basis of a more realistic theoretical model which includes second-nearest-neighbor interactions and electronic polarizability.

The model to be employed is the SM^{3,4} in the version used before by Peckham²¹ for calculating the phonon dispersion relations in MgO. It takes into account general first- and axially symmetric second-nearest-neighbor interaction and includes the polarizability of the anions only. The parameters of the model are determined from experimental values of elastic, dielectric, and optical constants and their dependence on pressure. The mode γ 's, the Grueneisen function $\gamma(T)$, and the moments $\gamma(n)$ will be calculated (a) for this model, (b) for the RIM corresponding to first-nearest-neighbor central-force interaction only, and (c) for a modified rigid-ion model (MRIM) based on general first-nearest-neighbor and axially symmetric second-nearest-neighbor interaction. The quasi-harmonic approximation will be used, and anharmonic effects will be partly eliminated by referring experimental and theoretical quantities to constant volume corresponding to $T = 0$ °K.

II. THEORETICAL MODELS

Since theoretical calculations based on various forms of the SM have been very successful in describing experimentally determined phonon dispersion curves for alkali halides³⁻⁶ and MgO,²¹ and since notable improvements over the RIM were obtained, it is to be expected that the SM will be a good basis for calculating the pressure dependence of phonon frequencies, or mode γ 's, and the macroscopic Grueneisen parameter as well. This has been confirmed for nine alkali halides and for MgO for the special case of the optical modes at

the zone center and the acoustical and optical modes at the [100] Brillouin-zone boundary.²² The present paper is an extension of this previous work to the calculation of the mode γ 's in the entire Brillouin zone and of the mode average required for the Grueneisen function $\gamma(T)$. The same theoretical model will be used as before.^{21,22} It takes into account general first-nearest-neighbor and axially symmetric second-nearest-neighbor interaction, and includes the polarizability of the anion only. On the assumption that the repulsive forces act through the shells only, there are six independent parameters which are determined from experimental values of the three elastic constants c_{11} , c_{12} , c_{44} from the static and optical dielectric constants ϵ_0 and ϵ_∞ , respectively, and from the TO frequency ω_0 . The explicit equations have been given before.^{3,4,21,22} For the calculation of the pressure dependence of the frequencies the pressure dependence of only five parameters is taken into account and determined from experimental values of the pressure derivatives of c_{11} , c_{12} , c_{44} , ϵ_0 , and ϵ_∞ . One of the parameters, the core-shell constant determining the electronic polarizability, is assumed to be independent of pressure.²² Since the pressure dependence of the shell charge is taken into account, this assumption does not imply that the electronic polarizability is constant. Good agreement was found between experimental and theoretical data for the pressure dependence of the TO frequency²² which suggests that this assumption is approximately valid.

be carried out for the RIM, with first-nearest-neighbor central-force interaction (Kellermann model) and for the MRIM with general first-nearest-neighbor and axially symmetric second-nearest-neighbor interaction, but no electronic polarizability included. For the RIM the third derivative of the interatomic potential is determined from

TABLE I. Elastic constants^a (in 10^{12} dyn/cm²) and their pressure derivatives^b at room temperature and absolute-zero temperature.

$T(^{\circ}\text{K})$	c_{11}^s	c_{12}^s	c_{44}	$\left(\frac{\partial c_{11}^s}{\partial p}\right)_T$	$\left(\frac{\partial c_{12}^s}{\partial p}\right)_T$	$\left(\frac{\partial c_{44}}{\partial p}\right)_T$
300	0.4870	0.1311	0.1266	11.66	2.08	0.37
0	0.5733	0.1122	0.1331	11.62	1.91	0.29

^aJ. T. Lewis, A. Lehozky, and C. V. Briscoe, Phys. Rev. **161**, 877 (1967).

^bCalculated from the values of $(\partial C_{ijkl}^s/\partial p)_T$ given by R. A. Bartels and D. Schuele [J. Phys. Chem. Solids **26**, 537 (1965)] for 195 and 295 °K by fitting the partial contractions of third-order elastic constants C_{ijklmn} $= -3B^T[(\partial C_{ijkl}^s/\partial p) - \delta_{ij}\delta_{kl} + \delta_{il}\delta_{jk} + \delta_{ik}\delta_{jl}]$ (all quantities in tensor notation; B^T = isothermal bulk modulus) to Eq. (13.12) of Ref. 15 with the energy function according to the Debye theory.

TABLE II. Static dielectric constant ϵ_0 and its relative pressure derivative $\epsilon'_0 = (1/\epsilon_0)(\partial\epsilon_0/\partial p)_T$ (in 10^{-12} cm²/dyn), optical refractive index $n = \sqrt{\epsilon_\infty}$ and its dimensionless pressure derivative $n' = B^T(\partial n/\partial p)_T$ (at $\lambda = 5893$ Å; B^T isothermal bulk modulus), ω_0 (in 10^{13} sec⁻¹), and nearest-neighbor distance r_0 (in Å) at room temperature and at absolute-zero temperature.

$T(^{\circ}\text{K})$	ϵ_0	ϵ'_0	n	n'	ω_0	r_0
300	5.909 ^a	-10.10 ^a	1.526 ^b	0.28 ^c	3.09 ^d	2.814 ^e
0	5.45 ^d	-9.2 ^f	1.533 ^d	0.28 ^g	3.35 ^d	2.793 ^h

^aB. W. Jones, Phil. Mag. **16**, 1085 (1967).

^bG. O. Jones, D. H. Martin, P. A. Mawer, and C. H. Perry, Proc. Roy. Soc. (London) **A261**, 10 (1961).

^cK. Vedam and E. D. D. Schmidt, Phys. Rev. (to be published).

^dR. P. Lowndes and D. H. Martin, Proc. Roy. Soc. (London) **A308**, 473 (1969).

^eM. Born and K. Huang, *Dynamical Theory of Crystal Lattices* (Oxford U. P., Oxford, England, 1953), p. 26.

^fRoom-temperature value from R. P. Lowndes and D. H. Martin, Proc. Roy. Soc. (London) **A316**, 351 (1970).

^gRoom-temperature value from Ref. c.

^hG. K. White, Proc. Roy. Soc. (London) **A286**, 204 (1965).

the pressure derivative of the bulk modulus, and the pressure derivatives of the general coupling parameters of the MRIM are determined from the pressure derivatives of the elastic constants.

The input data for NaCl are listed in Tables I and II for both room temperature and absolute-zero temperature. Calculations have been carried out for both sets of data in order to investigate the error incurred by determining the parameters of the model from room-temperature data. For c_{11} , c_{12} , c_{44} , ϵ_0 , ϵ_∞ , and ω_0 all input data given for $T = 0$ °K are experimental values. The pressure derivatives of c_{11} , c_{12} , and c_{44} were extrapolated to $T = 0$ °K from data at 295 and 195 °K.²³ The pressure derivatives of ϵ_0 and ϵ_∞ were assumed as constant. Since the temperature dependence of these pressure derivatives is only small^{24,25} this should involve an error of a few percent only. It should be noted, however, that even for constant pressure derivatives the mode γ 's turn out to change as much as 10–20% from 0 to 300 °K since they depend also on the temperature-dependent zero-pressure values of the input data. For the atomic masses the same values as listed in Table I of Ref. 22 have been used in the present paper.

III. MODE γ 's

The microscopic Grueneisen parameters (mode γ 's) are defined^{26,7,8} as the logarithmic volume derivative of the vibrational frequency $\omega_\lambda(\vec{q})$ of wave vector \vec{q} and branch λ :

$$\gamma_\lambda(\tilde{q}) = - \left(\frac{\partial \ln \omega_\lambda(\tilde{q})}{\partial \ln V} \right)_T \quad (3.1a)$$

Converting the volume derivative into a pressure derivative gives

$$\gamma_\lambda(\tilde{q}) = \frac{B^T}{\omega_\lambda(\tilde{q})} \left(\frac{\partial \omega_\lambda(\tilde{q})}{\partial p} \right)_T \quad (3.1b)$$

Here B^T denotes the isothermal bulk modulus. The pressure derivatives of the vibrational frequencies will be derived below from the eigenvalues of the dynamical matrix for the SM by means of the perturbation expansion with respect to pressure.

A. Perturbation Expansion for SM

The time-independent equations of motion for the SM are, in reciprocal space, given by⁴

$$\begin{aligned} \underline{M} \underline{\Lambda} \underline{U} &= \underline{A} \underline{U} + \underline{B} \underline{W}, \\ \underline{O} &= \underline{B}^* \underline{U} + \underline{D} \underline{W}. \end{aligned} \quad (3.2)$$

The coupling matrices \underline{A} , \underline{B} , and \underline{D} are $3s \times 3s$ matrices where s denotes the number of ions per unit cell. They can be separated into repulsive and Coulomb interaction terms according to⁴

$$\begin{aligned} \underline{A} &= \underline{R} + \underline{Z} \underline{C} \underline{Z}, \\ \underline{B} &= \underline{T} + \underline{Z} \underline{C} \underline{Y}, \\ \underline{D} &= \underline{S} + \underline{K} + \underline{Y} \underline{C} \underline{Y}. \end{aligned} \quad (3.3)$$

The mass matrix \underline{M} is a diagonal matrix of order $3s$, and \underline{U} and \underline{W} are $3s$ -dimensional eigenvectors denoting the displacements of the cores and the relative shell-core displacement, respectively. All quantities depend on the wave vector \tilde{q} , and the eigenvalues $\Lambda = \omega^2$ and the eigenvectors \underline{U} and \underline{W} in addition on the branch index $\lambda = 1, 2, \dots, s$.

As described above, the various force constants involved in these coupling matrices are derived from experimental values of the elastic constants c_{11} , c_{12} , c_{44} of the dielectric constants ϵ_0 and ϵ_∞ , and of the infrared dispersion frequency ω_0 . The pressure derivatives of the eigenfrequencies can be found in terms of these quantities and their pressure derivatives by treating the pressure p as a perturbation. Expanding the various matrices and vectors according to

$$\begin{aligned} \underline{A} &= \underline{A}_0 + \underline{A}_1 p + \left(\frac{1}{2} \underline{A}_2\right) p^2, \\ \underline{B} &= \underline{B}_0 + \underline{B}_1 p + \left(\frac{1}{2} \underline{B}_2\right) p^2, \\ \underline{D} &= \underline{D}_0 + \underline{D}_1 p + \left(\frac{1}{2} \underline{D}_2\right) p^2, \\ \underline{U} &= \underline{U}_0 + \underline{U}_1 p + \left(\frac{1}{2} \underline{U}_2\right) p^2, \\ \underline{W} &= \underline{W}_0 + \underline{W}_1 p + \left(\frac{1}{2} \underline{W}_2\right) p^2, \\ \Lambda &= \Lambda_0 + \Lambda_1 p + \left(\frac{1}{2} \Lambda_2\right) p^2, \end{aligned} \quad (3.4)$$

substituting Eq. (3.4) into Eq. (3.2), and collecting terms of the same power in p , one obtains for the zero-order equations

$$\begin{aligned} \underline{M} \underline{\Lambda}_0 \underline{U}_0 &= \underline{A}_0 \underline{U}_0 + \underline{B}_0 \underline{W}_0, \\ 0 &= \underline{B}_0^* \underline{U}_0 + \underline{D}_0 \underline{W}_0. \end{aligned} \quad (3.5)$$

The first-order perturbation equations are given by

$$\begin{aligned} \underline{M} \underline{\Lambda}_1 \underline{U}_0 + \underline{M} \underline{\Lambda}_0 \underline{U}_1 &= \underline{A}_1 \underline{U}_1 + \underline{B}_1 \underline{W}_0 + \underline{B}_0 \underline{W}_1, \\ 0 &= \underline{B}_1^* \underline{U}_0 + \underline{B}_0^* \underline{U}_1 + \underline{D}_1 \underline{W}_0 + \underline{D}_0 \underline{W}_1. \end{aligned} \quad (3.6)$$

Eliminating \underline{W}_0 and \underline{W}_1 from the two equations (3.5) and (3.6) gives

$$\begin{aligned} (\underline{M} \underline{\Lambda}_0 - \underline{A}_0 + \underline{B}_0 \underline{D}_0^{-1} \underline{B}_0^*) \underline{U}_1 \\ = (-\underline{M} \underline{\Lambda}_1 + \underline{A}_1 - \underline{B}_0 \underline{D}_0^{-1} \underline{B}_1^* - \underline{B}_1 \underline{D}_0^{-1} \underline{B}_0^* \\ + \underline{B}_0 \underline{D}_0^{-1} \underline{D}_1 \underline{D}_0^{-1} \underline{B}_0^*) \underline{U}_0. \end{aligned} \quad (3.7)$$

It can be easily seen from Eq. (3.7) that the first-order perturbation theory yields the perturbation to the frequencies belonging to the mode \tilde{q} , λ as

$$\begin{aligned} \Lambda_1(\tilde{q}, \lambda) &= \underline{U}_0^T(\tilde{q}, \lambda) (\underline{A}_1 - \underline{B}_0 \underline{D}_0^{-1} \underline{B}_1^* - \underline{B}_1 \underline{D}_0^{-1} \underline{B}_0^* \\ &+ \underline{B}_0 \underline{D}_0^{-1} \underline{D}_1 \underline{D}_0^{-1} \underline{B}_0^*) \underline{U}_0(\tilde{q}, \lambda). \end{aligned} \quad (3.8)$$

Because of $\Lambda(\tilde{q}, \lambda) = [\omega_\lambda(\tilde{q})]^2$, the mode γ 's according to (3.1b) become

$$\gamma_\lambda(\tilde{q}) = [B^T / 2\Lambda_0(\tilde{q}, \lambda)] \Lambda_1(\tilde{q}, \lambda). \quad (3.9)$$

B. Numerical Results and Discussion

The mode γ 's $\gamma_\lambda(\tilde{q})$ calculated from (3.9) for the RIM and for the SM with all input data taken at $T = 0^\circ \text{K}$ are shown in Fig. 1 as functions of the wave vector for the directions [100], [110], and [111].²⁷ The most obvious differences between the two sets of curves are that the total spread is about 25% smaller for the SM, and that the mode γ 's of the two TA branches in [100] and [110] which correspond in the long-wavelength limit to the shear modulus c_{44} are raised from negative to positive values. Also the TA branch in [110] which corresponds in the long-wavelength limit to the shear modulus $c_s = \frac{1}{2}(c_{11} - c_{12})$ is lower for the SM. The only other branch that is higher for the SM is the LA branch in [111]. Most other branches lie either lower in the SM or remain essentially unchanged (such as the LO branch in [111]). For several branches qualitative differences occur. The maximum of the LA branch in [110] and the minimum in the LO branch in [100] are absent for the SM, but for the TO₂ branch a deep and sharp minimum occurs at the [110] Brillouin-zone boundary. In

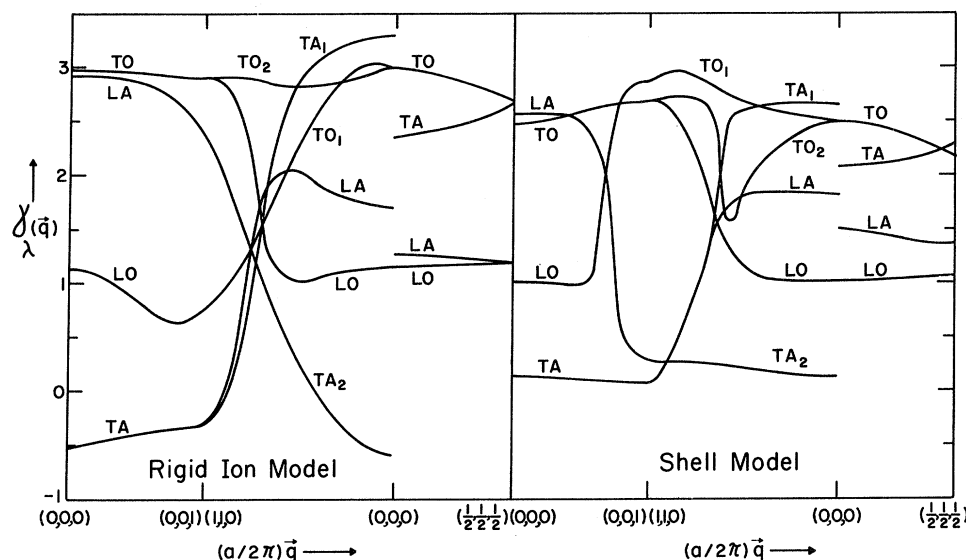


FIG. 1. Mode γ 's of NaCl vs wave vector for RIM and for SM at $T=0^\circ\text{K}$.

several cases large differences in the slope of the curves are present, such that the SM curves lie higher near the zone center, and lower near the zone edge, or vice versa, such as for the TA_2 branch in [110] and the TO_1 branch in [110].

It would be difficult to give a detailed physical explanation of the resulting differences in terms of the differences of the two models, i.e., the pressure dependence of the noncentral force and second-nearest-neighbor interaction and of the electronic polarizability. Since it is known that the pressure derivative $(\partial c_{44}/\partial p)$ increases and $(\partial c_s/\partial p)$ decreases with increasing second-nearest-neighbor interaction in alkali halides^{19,20} it is certain, however, that inclusion of the second-nearest-neighbor interaction raises the TA branch in [100] and the TA_2 branch in [110] near the zone center, and that it lowers the TA_1 branch near the zone center.

In order to determine the effect of the temperature of the input data, the mode γ 's were also calculated for both models with the room-temperature input data of Tables I and II. While in general the shape of the curves was not changed very much, the branches corresponding to large mode γ 's were displaced toward higher values.

IV. THERMAL GRUENEISEN PARAMETER

The thermal (or macroscopic) Grueneisen parameter γ is defined as²⁶

$$\gamma = \beta B^s / \rho c_p, \quad (4.1)$$

where β is the volume thermal expansion coefficient, B^s the adiabatic bulk modulus, ρ the density, and c_p the specific heat for constant pressure. Since all quantities in (4.1) are referred to zero pressure and are temperature dependent, the Grueneisen function $\gamma(T)$ is referred to constant pressure, i.e., $p=0$. In order to facilitate comparison with the theoretical results it is advantageous to refer all quantities to constant volume V_0 , which will be taken as the volume at $T=0^\circ\text{K}$. Following Barron *et al.*⁹ the linear approximation will be used:

$$\gamma(V, T) = \gamma(V_0, T) \left[1 + \left(\frac{\partial \ln \gamma}{\partial \ln V} \right)_T \frac{(V - V_0)}{V_0} \right]. \quad (4.2)$$

Here V denotes the volume at temperature T . The volume derivative $(\partial \ln \gamma / \partial \ln V)_T$ can be expressed through thermodynamic identities in the form^{9,28,29}

$$\left(\frac{\partial \ln \gamma}{\partial \ln V} \right)_T = 1 + \left\{ \delta_s + \gamma - \left(\frac{\partial B^s}{\partial p} \right)_T + (R-1) \left[\left(\frac{\partial \beta}{\partial T} \right)_p / \beta^2 - \left(\frac{\partial \ln c_p}{\partial T} \right)_p / \beta \right] \right\} / R, \quad (4.3)$$

where $\delta_s = -(\partial \ln B^s / \partial T)_p / \beta$ is the Anderson-Grueneisen parameter³⁰ and $R = 1 + \gamma \beta T$. Although the quantity (4.3) should be evaluated at $V = V_0$ and at temperature T the constant value corresponding to volume V and temperature 300°K should be used since the difference is a quantity of higher order.

The value calculated from the data in Tables I and II and from the temperature derivatives of B^s , β , and c_p listed in Ref. 31 is $(\partial \ln \gamma / \partial \ln V)_T = 1.52$. This value is much larger than the value of 0.3 given by Barron *et al.*,⁹ but it is of the same order as the values found for all other alkali halides calcu-

lated from Eq. (4.3) with the thermal and thermo-elastic data listed in Ref. 31. It agrees also approximately with the value of 1.46 calculated by Bassett *et al.*³² from a formula similar to (4.3). In that formula the term $(\partial\gamma/\partial T)_V$, which may be expected to be very small, has been neglected. Since the conversion of γ to constant volume is found to amount at most to 3%, one may assume that the value of 1.52 is sufficiently accurate for the desired purpose.

For the comparison with the theoretical data the thermal expansion data of White,¹⁷ who presents his results also directly in the form of values for γ , will be used. Since these values are calculated from bulk-modulus data of Overton and Swim³³ they were converted to the bulk-modulus data of Lewis *et al.*³⁴ used in the present calculations. This correction amounts to an increase of γ by 2.1% at room temperature, by a maximum of 4.2% at 150 °K, and by 3.3% at and below 80 °K.

In Fig. 2 these converted experimental data of White^{17,35} are shown as a function of temperature for constant pressure and for constant volume V_0 . A Debye temperature of 320.9 °K as calculated from the elastic constant data of Table I for 0 °K has been used for the lower scale of the abscissa in units of T/Θ . The difference between the two sets of data decreases with decreasing temperature, and below about 90 °K they become indistinguishable in Fig. 2. The experimental data of Meincke and Graham¹¹ agree closely with those of White¹⁷ if the same specific-heat data are used in their evaluation.⁹ They are therefore not included in Fig. 2. Additional experimental thermal expansion data are available from Rubin *et al.*^{14a} and from Yates and Panter³⁶ which agree well with White's data at high temperature but show significant deviations below 25 and 60 °K, respectively. The probable total error of the Grueneisen parameter estimated by Barron *et al.*⁹ from the thermal expansion data of Rubin *et al.* and of White¹⁴ amounts to 11% for $T < 10$ °K, 6% for $10 < T < 20$ °K, and 3% for $T > 20$ °K, with most of the uncertainty at high temperature arising from the bulk modulus.⁹ These figures should approximately also indicate the error of the Grueneisen parameter data of White¹⁷ in Fig. 2.

In the quasiharmonic approximation¹⁵ the thermal Grueneisen parameter is for constant volume given by the weighted average of the mode γ 's,²⁶

$$\gamma = \frac{\sum_{\lambda} c_{\lambda}(\bar{q}, T) \gamma_{\lambda}(\bar{q}, T)}{\sum_{\lambda} c_{\lambda}(\bar{q}, T)}, \quad (4.4)$$

where the weight factors $c_{\lambda}(\bar{q}, T)$ are given by the Einstein specific heat of the mode \bar{q}, λ . The mode average (4.4) has been performed for the RIM and the SM as explained in Sec. II with the mode γ 's and the frequencies calculated from the input data of Tables I and II for $T = 0$ and 300 °K. In addition

the calculations were performed for the MRIM with elastic constants at $T = 0$ °K used as input. All calculations were made with double precision on an IBM 360. The summation in (4.4) was extended over 48 points in the basic triangular pyramid of volume $\frac{1}{48}$ of the Brillouin zone, corresponding to a mesh width of $\Delta q_i = 0.1$ ($2\pi/a$). In order to check the accuracy obtainable with this coarse mesh width the calculations were repeated for the SM with 0 °K input data with a mesh width of $\Delta q_i = 0.05$ ($2\pi/a$), corresponding to 260 points in the basic triangular pyramid. The results for γ were found to differ from each other at 300 °K by 0.002, at 200 °K by 0.003, at 100 °K by 0.005, at 20 °K by 0.008, at 10 °K by 0.018, and at 6 °K by 0.057. One may therefore estimate that the accuracy of all calculations is better than 1% above 20 °K, and about 2% above 10 °K, and that larger uncertainties arise at still lower temperature.

All theoretical results are plotted in Fig. 2 as a function of temperature. For the SM calculations with 0 °K input only the results for the finer of the two mesh widths are shown. In addition, the low-temperature γ_0 as calculated from the elastic data of Table I by using the method of Brugger and Fritz³⁷ is indicated for the two SM calculations. Since the results for the MRIM are based on the same elastic constant data as the SM results with 0 °K input, the two curves should approach the same low-temperature limit γ_0 . Different values for γ_0 are obtained, however, for the RIM results because the RIM cannot exactly account for the elastic constants and their pressure derivatives. The values of γ_0 obtained for the RIM with input data at 300 and 0 °K are 1.074 and 0.911, respectively. At low temperature ($T/\Theta < 0.02$) the theoretical data are

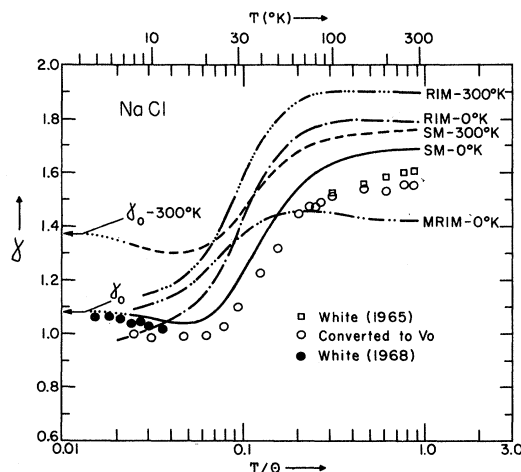


FIG. 2. Comparison of theoretical Grueneisen function $\gamma(T)$ of NaCl for RIM, MRIM, and SM with experimental data of White (Refs. 17 and 35) (constant pressure \square ; constant volume V_0 \circ , \bullet).

not accurate enough to establish the exact shape of the $\gamma(T)$ curve because too few points are included in the summation in (4.4) over the center region of the Brillouin zone which contains the only modes that are excited at low temperature. Therefore the conjectured course of $\gamma(T)$ at low temperature has been dotted in Fig. 2 for the two SM curves.

It is apparent that the SM curve with input data referred to $T=0^\circ\text{K}$ shows the best agreement with the experimental data, both in absolute magnitude and in the shape of the curve. At low temperatures this theoretical curve is too high by about 0.06 (6%), and at high temperature by about 0.13 (8.4%). Below 22°K the theoretical curve drops below the low-temperature elastic limit of 1.08, and a shallow minimum of depth 0.06 occurs at about $T/\Theta=0.045$ ($T=15^\circ\text{K}$). Apparently this minimum is caused by the decrease of the mode γ of the TA mode in [100] from 0.125 at the zone center to 0.055 at the zone edge (Fig. 1). At 15°K the specific-heat contribution from the TA mode at the [100] zone edge amounts to only 20% of a fully excited mode, but because of the large density of states at the zone edge, the total contribution of all modes near the [100] zone edge to the thermal Grueneisen parameter may indeed be larger than that from the long-wavelength modes. The theoretical curves for the RIM seem to decrease monotonically with decreasing temperature and approach the low-temperature elastic limit of 1.074 (RIM-300 $^\circ\text{K}$) and 0.911 (RIM-0 $^\circ\text{K}$) without any indication of a minimum. This confirms the conclusions of Barron and Batana¹⁸ that for the RIM³⁸ no significant minimum (of depth 0.1 or larger) should occur. Contrary to the results for the RIM the data presented here for the SM indicate, however, the existence of a shallow minimum³⁵ of depth 0.06.

Possible reasons for the discrepancies between the SM curve referred to $T=0^\circ\text{K}$ and the experimental data are the experimental error of the Grueneisen parameter, the limitations of the SM itself, and the experimental error of the input data of Tables I and II. Since the conversion to constant volume amounts only to a small correction of maximally 3.2% one might expect that anharmonic contributions of the zero-point motion occurring for constant volume are still smaller. As Thomsen³⁹ has recently shown these contributions correspond to fifth- and higher-order anharmonic terms, and it is therefore very unlikely that they are present below the Debye temperature and contribute substantially to the discrepancy between experimental and theoretical data.

The theoretical curve based on the RIM at 0°K lies at temperatures higher than 12°K above the SM curve and shows a steeper increase with increasing temperature and reaches a constant value at a much lower temperature than the SM curve.

The high-temperature limit is higher by an amount of 0.11 than the SM curve and the deviation from the experimental data is twice as large as for the SM.

While the curves for the RIM show a weak maximum at about 140°K , the curve based on the MRIM with input for 0°K shows a pronounced maximum of 1.46 at 70°K . The MRIM curve rises much more slowly with increasing temperature than the SM and RIM curves and lies at low temperatures ($<50^\circ\text{K}$) above, and at high temperature below, the SM curve. The high-temperature limit is smaller by 0.13 than the experimental data.

Comparing the three models considered shows that by including first-nearest-neighbor noncentral and second-nearest-neighbor central forces the value of γ is increased at low temperatures and decreased at high temperatures, but that including the polarizability of the ions has the opposite effect. At low temperature (below 15°K) the two contributions cancel so that the RIM is a better approximation. At higher temperatures the two contributions cancel only partly and the first effect dominates. This cancellation of the various contributions appears to be the main reason why the simple RIM was believed to be quite adequate for describing the temperature dependence of the thermal Grueneisen parameter. In addition, the surprisingly good agreement found by several authors^{10,11,18} seems to have been caused by the fact that the repulsive parameters were determined from the long-wavelength limit of the TO frequency, and not from the bulk modulus, and that the equilibrium condition was ignored, so that these data refer to a crystal under hydrostatic compression.

The curves calculated for the SM and for the RIM from room-temperature input data are found to lie considerably higher than the corresponding curves referred to 0°K . In order to compare these data with experimental results the latter should be referred, however, to the volume V_{300} at 300°K . This would raise all experimental points referred to V_0 at 0°K by an amount of 0.05 which is smaller than the differences between the two sets of theoretical curves referred to $T=300$ and 0°K . This discrepancy illustrates the importance of eliminating thermal effects by referring the input data to $T=0^\circ\text{K}$.

V. VOLUME DERIVATIVES OF MOMENTS OF THE FREQUENCY SPECTRUM

Barron *et al.*⁹ have shown that the temperature dependence of the Grueneisen function $\gamma(T)$ can be used to determine for integer values of n the volume derivatives of the moments $\langle\omega^n\rangle$ of the frequency spectrum of the lattice vibrations which are given by

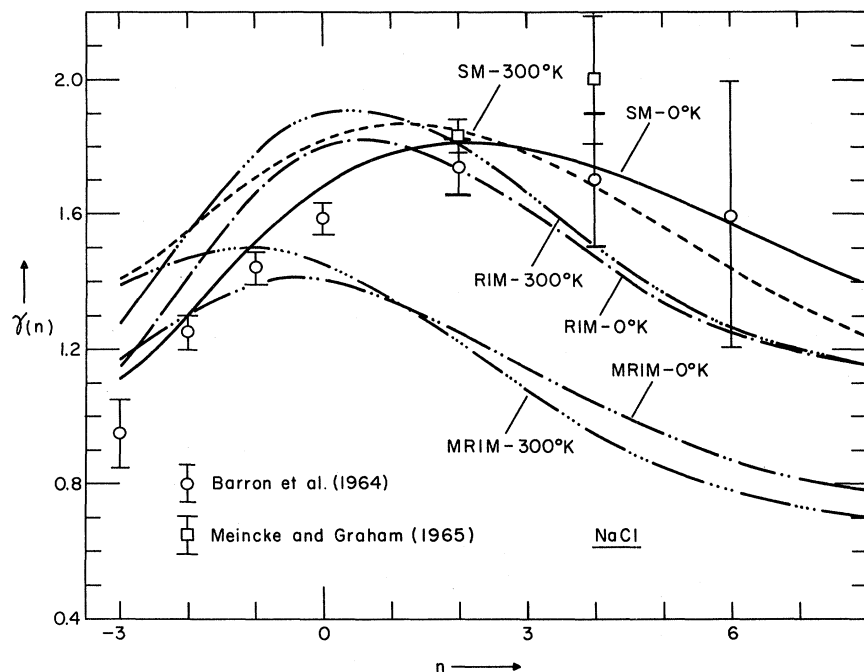


FIG. 3. Volume derivations $\gamma(n)$ of moments of frequency spectrum vs n for NaCl from theoretical models and from experimental data of Rubin *et al.* and White (Ref. 14), Barron *et al.* (Ref. 9), and Meincke and Graham (Ref. 11).

$$\gamma(n) = -\frac{1}{n} \left(\frac{\partial \ln \langle \omega^n \rangle}{\partial \ln V} \right)_T. \quad (5.1)$$

After carrying out the differentiation this quantity can also be written in view of (3.1) as

$$\gamma(n) = \frac{\sum_{\vec{q}\lambda} [\omega_{\lambda}(\vec{q})]^n \gamma_{\lambda}(\vec{q})}{\sum_{\vec{q}\lambda} [\omega_{\lambda}(\vec{q})]^n}. \quad (5.2)$$

The advantage of these quantities over the Grueneisen function $\gamma(T)$ is that they are temperature independent and directly related to the properties of the frequency spectrum. They can also be obtained from the coupling parameters without solving the secular equation.

The quantity $\gamma(n)$ has been calculated from (5.2) by direct summation for the three models discussed above, both for room-temperature and for zero-temperature input data, for integer values of n from -3 to $+8$. The results are compared in Fig. 3 with the data calculated by Barron *et al.*⁹ from experimental thermal expansion data of Rubin *et al.* and White,¹⁴ and with the data calculated by Meincke and Graham¹¹ from their own experimental data. The experimental data in Fig. 3 are not referred to constant volume V_0 , and are based on different bulk-modulus data than those used in the theoretical calculations. No attempt has been made, however, to correct for these differences since they are smaller than the estimated experimental errors shown.

It is apparent that of all theoretical curves shown the SM curve with zero-temperature input agrees best with the experimental data. For positive values of n the agreement is within the large esti-

mated experimental error, but for negative values of n the deviations are larger. These discrepancies are probably due to the limitations of the theoretical model and the experimental error of the input data.

VI. SUMMARY AND CONCLUSIONS

It has been shown that a six-parameter SM, in which five parameters are taken as pressure dependent, is capable of reproducing the Grueneisen function $\gamma(T)$ below and up to the Debye temperature within 6–8%. The discrepancy seems to indicate the limited accuracy with which the parameters of the model which describe the interatomic forces can be determined from experimental elastic, optical, and dielectric data, even if these are determined at or extrapolated to absolute-zero temperature. Referring the input data to $T = 0^\circ\text{K}$ has been found to be important. Conversion to constant volume decreases the experimental data at high temperature and increases the discrepancy with the theoretical data from 5 to 8%. On the basis of the theoretical results it is also possible to expect a shallow minimum of the Grueneisen function near 15°K .

It has also been shown that the RIM of Kellermann, if used properly in connection with the equilibrium condition and the bulk modulus, is much less satisfactory than the SM used here. Qualitatively, however, it does represent the general shape of the $\gamma(T)$ curve quite well. This

is shown to arise from the partial cancellation of two errors of opposite sign due to the omission of second-nearest-neighbor repulsion and electronic polarizability.

ACKNOWLEDGMENT

The authors would like to thank Dr. S. Y. La for writing the computer program for calculating the elastic limit of the Grueneisen parameter.

*Work supported by the National Science Foundation.

†Present address: Argonne National Laboratory, Argonne, Ill. 60439.

¹E. W. Kellermann, Phil. Trans. Roy. Soc. London **238**, 513 (1940).

²E. W. Kellermann, Proc. Roy. Soc. (London) **A238**, 17 (1941).

³A. D. B. Woods, W. Cochran, and B. N. Brockhouse, Phys. Rev. **119**, 980 (1960); R. A. Cowley, W. Cochran, B. N. Brockhouse, and A. D. B. Woods, *ibid.* **131**, 1030 (1963).

⁴R. A. Cowley, Proc. Roy. Soc. (London) **A268**, 121 (1962).

⁵A. M. Karo and J. R. Hardy, Phys. Rev. **129**, 2024 (1963); **141**, 696 (1966).

⁶V. Nüsslein and U. Schröder, Phys. Status Solidi **21**, 309 (1967).

⁷M. Blackmann, Proc. Phys. Soc. (London) **B70**, 827 (1957); Phil. Mag. **3**, 831 (1958).

⁸T. H. K. Barron, Ann. Phys. (N. Y.) **1**, 77 (1957).

⁹T. H. K. Barron, A. J. Leadbetter, and J. A. Morrison, Proc. Roy. Soc. (London) **A279**, 62 (1964).

¹⁰M. Arenstein, R. D. Hatcher, and J. Neuberger, Phys. Rev. **132**, 73 (1963).

¹¹P. P. M. Meincke and G. M. Graham, Can. J. Phys. **43**, 1853 (1965).

¹²G. C. Fletcher, Australian J. Phys. **12**, 237 (1959); D. G. M. Powell and G. C. Fletcher, *ibid.* **18**, 205 (1965).

¹³G. L. Morley, J. Chem. Phys. **51**, 2336 (1969).

¹⁴(a) T. Rubin, H. L. Johnston, and H. W. Altman, J. Phys. Chem. **65**, 65 (1961). (b) G. K. White, *Proceedings of the VIII International Conference on Low Temperature Physics* (Butterworths, London, 1963), p. 394.

¹⁵G. Leibfried and W. Ludwig, Solid State Phys. **12**, 275 (1961).

¹⁶E. R. Cowley and R. A. Cowley, Proc. Roy. Soc. (London) **A287**, 259 (1965).

¹⁷G. K. White, Proc. Roy. Soc. (London) **A286**, 204 (1965).

¹⁸T. H. K. Barron and A. Batana, Phys. Rev. **167**, 814 (1968).

¹⁹C. S. Smith, D. E. Schuele, and W. B. Daniels, in *Proceedings of the First International Conference on Physics of Solids at High Pressure*, edited by C. Tomizuka (Academic, New York, 1965), p. 496.

²⁰G. R. Barsch and H. E. Shull, Phys. Status Solidi **43**, 637 (1971).

²¹G. Peckham, Proc. Phys. Soc. (London) **90**, 657 (1967).

²²G. R. Barsch and B. N. N. Achar, Phys. Status

Solidi **35**, 881 (1969).

²³R. A. Bartels and D. E. Schuele, J. Phys. Chem. Solids **26**, 537 (1965).

²⁴B. W. Jones, Phil. Mag. **16**, 1085 (1967).

²⁵R. P. Lowndes and D. H. Martin, Proc. Roy. Soc. (London) **A316**, 351 (1970).

²⁶J. C. Slater, *Introduction into Chemical Physics* (McGraw-Hill, New York, 1939), p. 217.

²⁷The mode γ 's at the zone center and at the [100] zone boundary agree approximately with those reported in Table 2 of Ref. 22, the differences being due to the use of room-temperature input data and graphical differentiation with respect to pressure in Ref. 22. Also in Table 2 of Ref. 22 the values of the LO and LA mode γ 's at the [100] zone boundary have been inadvertently exchanged for NaCl.

²⁸G. R. Barsch, Phys. Status Solidi **19**, 129 (1967).

²⁹J. S. Yu, Appl. Sci. Res. **19**, 220 (1968).

³⁰O. L. Anderson, Phys. Rev. **144**, 553 (1966).

³¹G. R. Barsch and Z. P. Chang, Phys. Status Solidi **19**, 139 (1967).

³²W. A. Bassett, T. Takahashi, H. K. Mao, and J. S. Weaver, J. Appl. Phys. **39**, 319 (1968).

³³W. C. Overton and R. T. Swim, Phys. Rev. **84**, 758 (1951).

³⁴J. T. Lewis, A. Lehozky, and C. V. Briscoe, Phys. Rev. **161**, 877 (1967).

³⁵More recent measurements of G. K. White [in *Proceeding of the Eleventh International Conference on Low-Temperature Physics*, edited by J. F. Allen, D. M. Finlayson, and D. M. McCall (University of St. Andrews Printing Dept., St. Andrews, Scotland, 1969)] show a shallow minimum and give better agreement with the low-temperature elastic limit γ_0 and the theoretical SM data of Figs. 2 and 3. These more recent data of White have been added to Fig. 2 without making the small correction for the different bulk moduli.

³⁶B. Yates and C. H. Panter, Proc. Phys. Soc. (London) **80**, 373 (1962).

³⁷K. Brugger and T. Fritz, Phys. Rev. **157**, 524 (1967).

³⁸It should be noted that the RIM of Barron and Batana (Ref. 18) is not identical with the RIM model used here. Whereas Barron and Batana (Ref. 18) determine the third derivative of the nearest-neighbor repulsive potential from an exponential repulsive law, no potential form is assumed in the present model, and the third derivative of the repulsive potential is determined from the pressure derivative of the bulk modulus.

³⁹L. Thomsen, J. Phys. Chem. Solids (to be published).